Large magnetotunneling effect at low magnetic fields in micrometer-scale epitaxial $La_{0.67}Sr_{0.33}MnO_3$ tunnel junctions

Yu Lu, X. W. Li, G. Q. Gong, and Gang Xiao
Physics Department, Brown University, Providence, Rhode Island 02912

A. Gupta, P. Lecoeur, and J. Z. Sun
IBM Research Division, T. J. Watson Research Center, Yorktown Heights, New York 10698

Y. Y. Wang and V. P. Dravid
Materials Science and Engineering Department, Northwestern University, Evanston, Illinois 60208
(Received 8 July 1996)

We have used a self-aligned lithographic process to fabricate magnetic tunnel junctions of $La_{0.67}Sr_{0.33}MnO_3$ down to a few micrometers in size. We have obtained a magnetoresistance ratio as large as 83% at low magnetic fields of a few tens of Oe, which correspond to the coercivities of the magnetic layers. Transmission-electron-microscopy analysis has revealed the heteroepitaxial growth of the trilayer junction structure, $La_{0.67}Sr_{0.33}MnO_3/SrTiO_3/La_{0.67}Sr_{0.33}MnO_3$. We have observed current-voltage characteristics typical of electron tunneling across an insulating barrier. The large magnetoresistance is likely due to the nearly half-metallic electronic structure of the manganites. [S0163-1829(96)52636-6]

The magnetotransport properties of manganese perovskites have been the subject of intense research recently.[1–5] These oxides, $La_{1-x}D_xMnO_3$ (D=Ca, Sr, Ba, etc.), exhibit a large change in resistance when subject to a Tesla-range magnetic field, so large that this effect has been called ''colossal'' magnetoresistance (CMR). Essential to the physics of CMR is the existence of the mixed valence states of Mn^{3+} (fraction: $1-x$) and Mn^{4+} (fraction: x). Both ions possess a local spin ($S=3/2$) from their low-lying t_{2g}^3 orbitals. In addition, Mn^{3+} ($3d^4$) has an extra electron in the e_g orbital, which is responsible for conduction, whereas in Mn^{4+} ($3d^3$) this orbital is empty (i.e., having a hole). The spin of the e_g^1 electron in Mn^{3+} is ferromagnetically coupled to the local spin of t_{2g}^3 according to Hund's rule. It is this strong intra-atomic exchange that fosters the sensitivity with which the electron transport responds to a changing magnetic structure. In order to observe CMR, which occurs near the magnetic phase transition temperature (T_c), a large field of the order of Teslas is required since a low field would be insufficient to suppress the thermal magnetic disorder. Reducing the field scale in the magnetoresistance of manganites has been a major goal of many research groups.

One approach to reducing the field scale is to take advantage of the recent discovery of large magnetoresistance (MR) in magnetic tunnel junctions.[6–9] These are sandwiches of two magnetic layers separated by a thin insulating barrier. The tunneling resistance between the two magnetic layers depends on the relative orientation of the magnetizations in the layers. Recently, Sun *et al.*[9] have demonstrated large changes of about a factor of two in resistance at fields below 200 Oe in trilayers made of manganites and a $SrTiO_3$ barrier, when measured in the current-perpendicular-to-plane mode. However, the spin-dependent transport mechanism was not known and the microstructures of the trilayers were not characterized.

We have used the same approach to reduce the field scale of magnetotransport by fabricating and studying magnetic tunnel junctions using manganites. We will demonstrate that epitaxial junctions in the form of [(**top electrode**) $La_{0.67}Sr_{0.33}MnO_3$]/(**barrier**) $SrTiO_3$]/[(**bottom electrode**) $La_{0.67}Sr_{0.33}MnO_3$] or LSMO/STO/LSMO have been achieved as evidenced from the microstructures obtained from transmission electron microscopy (TEM). We have obtained a large magnetoresistance ratio of 83% at low fields of a few tens of Oe, which correspond to the coercivities of the magnetic layers. The mechanism of the spin-dependent transport is consistent with magnetotunneling. We have also measured the temperature dependence of the magnetotunneling effect.

We have grown the manganite tunnel junctions using a multitarget pulsed laser deposition system. STO was chosen as the insulating barrier because of its close lattice match with LSMO. The LSMO/STO/LSMO trilayers were grown *in situ* on optically polished (100)-oriented STO substrates. No subsequent thermal treatment was performed. Detailed synthesis conditions for the LSMO films can be found in Ref. 10. The thicknesses of both LSMO electrodes are about 500 Å , and the STO barrier thickness is in the range of 30–60 Å . Figure 1 is a high-resolution cross-sectional TEM lattice image of the interface region with the STO barrier (60 Å) in one of the junctions. All of the layers are heteroepitaxially aligned and sharp interfaces are observed between the STO and the LSMO layers. Scanning electron micrographs of the top surface of the trilayers have shown a smooth morphology with some particulates which are typical of laser ablation. Our results demonstrate that artificial stacking of LSMO and STO layers is possible for fabricating novel structures with potentially enhanced properties. The epitaxial layered structure is particularly useful for studying magnetotunneling because the effect is sensitive to the local electronic structure which is dependent on crystallographic orientations.

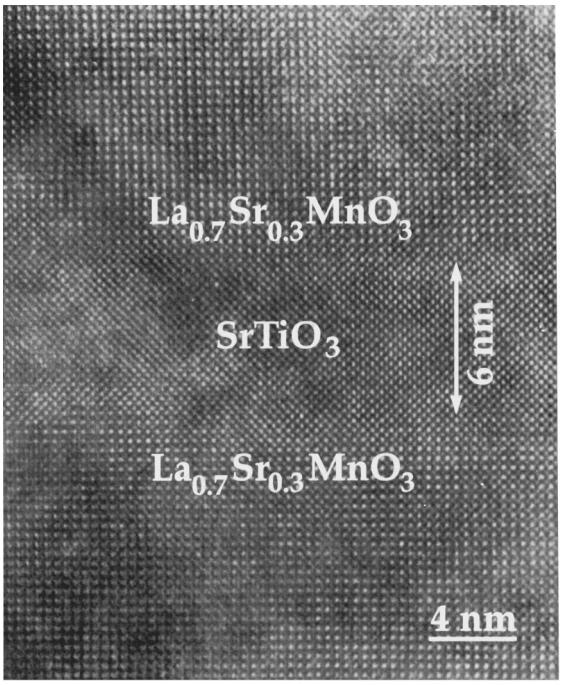

FIG. 1. High-resolution transmission electron micrograph of a cross-sectional lattice image obtained from a $La_{0.67}Sr_{0.33}MnO_3/SrTiO_3/La_{0.67}Sr_{0.33}MnO_3$ trilayer junction. The $SrTiO_3$ barrier thickness is 6 nm.

Figure 2 illustrates the fabrication process of micron-scale tunnel junctions. We have used a self-aligned lithographic process to pattern the device structures. The blank trilayer film (1×1 cm^2) [Fig. 2(a)] was first patterned by ion milling to define the base electrode [Fig. 2(b)]. The junction areas were defined by patterning the top electrodes. Ion milling was used for pattening the top electrode, with the etching

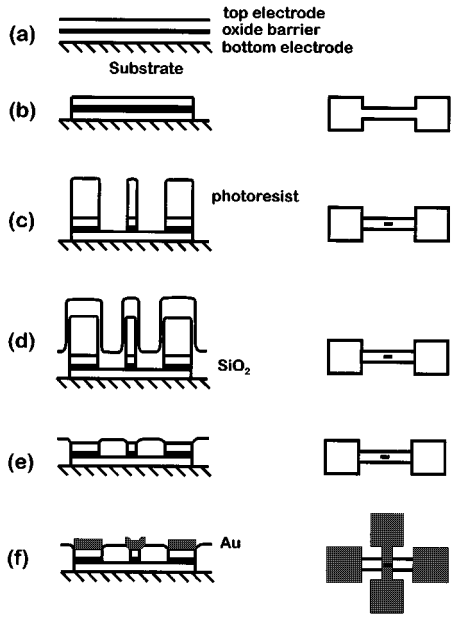

FIG. 2. Photolithographic patterning process for magnetic tunnel junctions. The left and right panels are cross sectional and planar views, respectively, of a magnetic tunnel junction (see text for explanation).

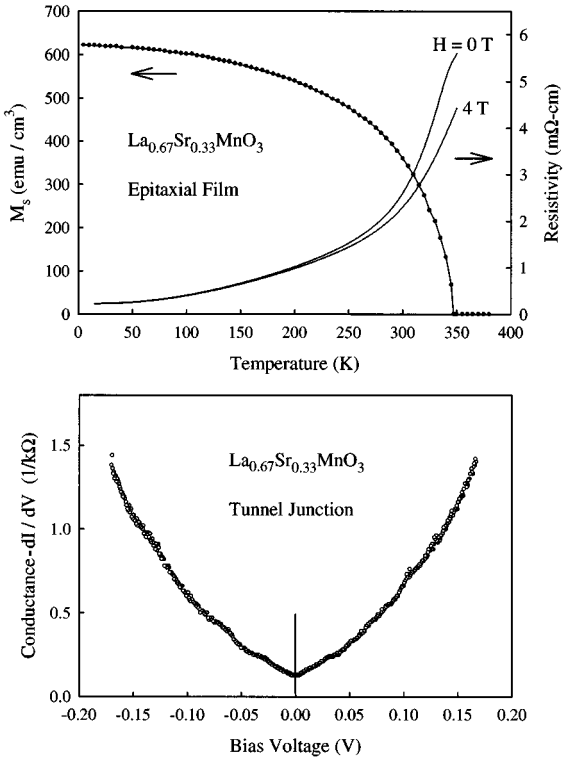

FIG. 3. (Top) the temperature dependence of the spontaneous magnetization and resistivity at zero and 4 T for a pure $La_{0.67}Sr_{0.33}MnO_3$ epitaxial thin film; (bottom) dynamic conductance dI/dV vs bias V at $T=4.2$ K of a tunnel junction with a rectangular 2.5×12.5 μm^2 top electrode.

timed to end at the top surface of the base electrode [Fig. 2(c)]. Next the junctions were coated with a 1500-Å layer of SiO_2 by sputtering [Fig. 2(d)]. The photoresist left after the previous ion milling step was used as the lift-off stencil to open self-aligned contact holes to the top electrodes [Fig. 2(e)]. Finally, a metalization layer of 3000-Å Au was deposited and patterned to make connection to the top electrodes [Fig. 2(f)]. We have used the four-probe technique to measure the I-V curves and the tunneling resistance as a function of field using conventional electronics. The magnetic properties were measured in a Quantum Design SQUID magnetometer.

To ascertain tunneling as the transport mechanism, we have measured the dynamic conductance (dI/dV) of a sample as a function of bias V, as shown in Fig. 3. The parabolic shape of the conductance curve is indicative of electron tunneling. We have also shown in Fig. 3 the spontaneous magnetization $[M_s(T)]$ and resistivities $[\rho_0(T),\rho_{4T}(T)]$ at zero field and 4 T of a pure LSMO film which was made under identical conditions as those used for making the junctions. The as-prepared LSMO film has a T_c of 347 K and a spontaneous magnetization of 622 emu/cm^3 at 4.2 K. The maximum change in resistance under a field of 4 T is about 31%, which occurs near T_c.

In Fig. 4, we show the field dependence of the tunneling resistance (R) and the MR ratio, $\Delta R/R_p$, of a junction (with area 2.5×12.5 μm^2) measured at $T=4.2$ K. Here R is measured at zero bias (i.e., $V=0$, the ac voltage for measurement is about 1 mV), and R_p is the saturated resistance when both

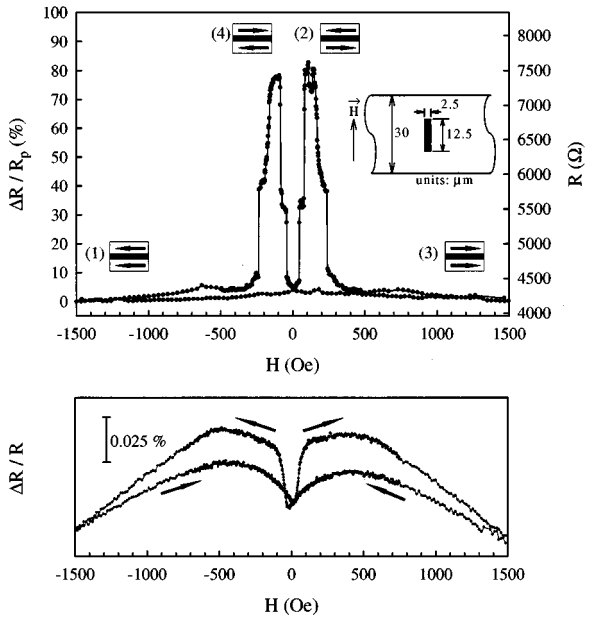

FIG. 4. (Top) magnetoresistance ratio $\Delta R/R_p$ and tunneling resistance R vs magnetic field at $T=4.2$ K for a tunnel junction with a rectangular 2.5×12.5 μm^2 top electrode. The field is applied along the easy axis of the top electrode. The moment orientations of both electrodes are shown at various fields, and the number preceding each orientation indicates the direction of the sweeping field; (bottom) $\Delta R/R$ vs field for the bottom electrode only. Note that MR is extremely small for the pure LSMO film in the field range of interest. The arrows show the direction of the sweeping field.

moments in the electrodes are parallel to each other at high fields. Also shown in the inset are the shapes of the top and bottom LSMO electrodes and the direction of the applied field which is along the magnetic easy axis of the top electrode. As the field is swept from -1500 to 1500 Oe, the junction first switches from R_p to a high $R_{\max}$ state at about $H_{c1}=56$ Oe. Then above $H_{c2}=160$ Oe, the junction starts to switch back to the R_p state. Reversing the field from 1500 Oe causes a similar sequence of switching processes. The maximum MR ratio, $(\Delta R/R_p)_{\max}=(R_{\max}-R_p)/R_p$, is about 83%, which is obtained at fields of a few tens of Oe. This is in sharp contrast to the high-field scale (Tesla range) required to observe the CMR in pure LSMO.

The sharp changes in R in Fig. 4 are associated with the moment reversals in the two electrodes. The switching fields, H_{c1} and H_{c2}, correspond to the magnetic coercivities of the bottom and the top electrodes, respectively. In the lower part of Fig. 4, we show the field dependence of MR for the bottom electrode only. At about H_{c1}, a fast change in MR is observed, indicating moment switching in the bottom electrode. A hysteresis loop measurement on bulk LSMO films also gives a coercivity of 48 Oe at 4.2 K. The other switching field, H_{c2}, is approximately the demagnetization field, $H_K=4\pi M_s d/w=156$ Oe, of the top rectangular electrode, where d is the film thickness (50 nm), w width (2.5 μm), and M_s magnetization (622 emu/cm^3).

In manganites, the conduction electrons are expected to be polarized due to the strong intra-atomic Hund's exchange. For spin-polarized tunneling, the tunneling current would be large (small) if the magnetizations of both electrodes are parallel (antiparallel) to each other. In other words, the tunneling resistance would be sensitive to the relative orientation of the moments in the electrodes. Indeed, at high fields, when the moments are aligned along the field direction, R attains a low value R_p. Whereas between H_{c1} and H_{c2}, R reaches the maximum value $R_{\max}$ because of the antiparallel orientations of the moments.

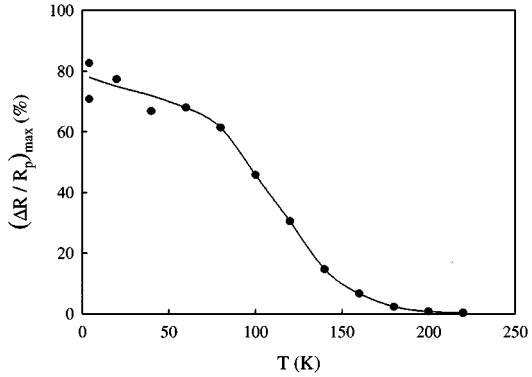

FIG. 5. Temperature dependence of the maximum magnetoresistance ratio $(\Delta R/R_p)_{\max}$ for the same sample used in Fig. 4. The field required to obtain $(\Delta R/R_p)_{\max}$ is always less than 110 Oe.

The magnetotunneling effect is caused by the asymmetry in the density of states (DOS) of the majority and minority bands in magnetic metals.[11–13] The larger the spin polarization, the larger the magnetotunneling effect. According to the model of spin-polarized tunneling,[11,12] the MR ratio for our structures is given by

$$(\Delta R/R_p)_{\max}=(R_{\uparrow\downarrow}-R_{\uparrow\uparrow})/R_{\uparrow\uparrow}=2P^2/(1-P^2), \quad (1)$$

$$P\equiv\frac{n_\uparrow-n_\downarrow}{n_\uparrow+n_\downarrow}, \quad (2)$$

where $R_{\uparrow\uparrow}$ and $R_{\uparrow\downarrow}$ are the resistances for the parallel and antiparallel M configurations, respectively (note $R_{\uparrow\uparrow}\equiv R_p$), P is the spin polarization parameter for LSMO, which has not been determined so far, and $n_\uparrow, n_\downarrow$ are the DOS of the majority and minority electrons. Recently, large MR of the order of 20% has been observed in several magnetic tunneling systems involving transition metals such as Co, Fe, and permalloy.[6–8] The magnitude of the MR is consistent with a typical $P\approx0.3$ in these metals.[11] In our LSMO/STO/LSMO junction, if we take $(\Delta R/R_p)_{\max}\approx83\%$, relation (1) leads to $P\approx0.54$ for LSMO. This value is much larger than that of a typical magnetic transition metal. Pickett and Singh[14] have calculated the band structures of $La_{1-x}Ca_xMnO_2$. Their results reveal that the manganite at $x=0.33$ resembles a half-metal, i.e., the minority DOS at the Fermi surface is very low. The calculated DOS leads to a $P\approx0.37$, which is smaller than our experimental $P\approx0.54$ for LSMO. This may be due to the different dopant used (i.e., Ca), or to the fact that the dopants are assigned to ordered lattice sites in theory rather than randomly distributed as in real materials.

We have also measured the magnetoresistance at various temperatures. In Fig. 5 we present the T dependence of the $(\Delta R/R_p)_{\max}$, which decreases steadily as temperature increases. The magnetotunneling effect seems to vanish at about $T\approx200$ K, which is lower than $T_c\approx346.5$ K for

LSMO. In comparison, we note that the CMR effect is most pronounced near T_c and it disappears as T approaches zero[2–4] (see Fig. 3). This is due to the enhanced magnetic scattering and the possible dynamic Jahn-Teller distortions near T_c.[15] The T dependence of the magnetotunneling effect is not understood at this moment. There are a few possible causes that need to be explored further. First, since magnetotunneling is primarily an interface effect, the intrinsically large spin-wave excitations at the interfaces[16] may lead to enhanced electron-magnon scattering, which can cause spin flipping. Secondly, the polarization parameter P itself in LSMO may be temperature dependent. Band theory calculations have shown that the electronic structures of manganites are intimately coupled to the underlying magnetic structure because of the large Hund's coupling.[14] The magnetic structure in manganites is expected to become very dynamic at elevated T, which could weaken the spin polarization. Another possible cause for the T dependence may be a less-than-ideal insulating barrier which may contain some impurities and defects. Further work is underway to clarify the thermal effect.

Finally, we note that Wiesendanger *et al.*[17] have reported the observation of vacuum tunneling of spin-polarized electrons from a ferromagnetic CrO_2 tip into Cr.

In conclusion, we have successfully fabricated micron-scale manganite heterojunctions which show large MR ratios of up to 83% in small external fields (tens of Oe). Cross-sectional TEM has shown good heteroepitaxy between the $La_{0.67}Sr_{0.33}MnO_3$ and the $SrTiO_3$ layers. The current-voltage characteristics are consistent with an electron tunneling mechanism. We have determined the electron polarization parameter (≈ 0.54) for $La_{0.67}Sr_{0.33}MnO_3$ using the model of spin-polarized tunneling. The magnetoresistance is found to be strongly dependent on temperature.

We wish to thank W. J. Gallagher, J. C. Slonczewksi, T. R. McGuire, S. S. P. Parkin, R. Laibowitz, C. Jahnes, P. L. Trouilloud, S. L. Brown, R. A. Altman, and J. C. Connolly for stimulating discussions and help. This work was supported by National Science Foundation Grants Nos. DMR-9414160 and DMR-9258306, IBM, and U.S. Department of Energy Grant No. DE-FG02-92ER45475.

[1] R. von Helmolt, J. Wecker, B. Holzapfel, L. Schultz, and K. Samwer, Phys. Rev. Lett. **71**, 2331 (1993).
[2] S. Jin, T. H. Tiefel, M. McCormack, R. A. Fastnacht, R. Ramesh, and L. H. Chen, Science **264**, 413 (1994).
[3] P. E. Schiffer, A. P. Ramirez, W. Bao, and S-W. Cheong, Phys. Rev. Lett. **75**, 3336 (1995).
[4] G. Q. Gong, C. L. Canedy, Gang Xiao, J. Z. Sun, A. Gupta, and W. J. Gallagher, Appl. Phys. Lett. **67**, 1783 (1995).
[5] Y. Tomioka, A. Asamitsu, Y. Moritomo, H. Kuwahara, and Y. Tokura, Phys. Rev. Lett. **74**, 5108 (1995); H. Kuwahara, Y. Tomioka, A. Asamitsu, Y. Moritomo, and Y. Tokura, Nature (London) **270**, 961 (1995).
[6] T. Miyazaki and N. Tezuka, J. Magn. Magn. Mater. **139**, L231 (1995).
[7] J. S. Moodera, L. R. Kinder, T. M. Wong, and R. Meservey, Phys. Rev. Lett. **74**, 3273 (1995).
[8] Yu Lu *et al.* (unpublished).
[9] J. Z. Sun, W. J. Gallagher, P. R. Duncombe, L. Krusin-Elbaum, R. A. Altman, A. Gupta, Yu Lu, G. Q. Gong, and Gang Xiao (unpublished).
[10] A. Gupta, T. R. McGuire, P. R. Duncombe, M. Rupp, J. Z. Sun, W. J. Gallagher, and Gang Xiao, Appl. Phys. Lett. **67**, 3494 (1995); P. LeCoeur, A. Gupta, P. R. Duncombe, G. Q. Dong, and Gang Xiao, J. Appl. Phys. **80**, 513 (1996).
[11] For a review of spin-polarized tunneling studies, see, e.g., R. Meservey and P. M. Tedrow, Phys. Rep. **239**, 174 (1994).
[12] M. Julliere, Phys. Lett. **54**, 225 (1975).
[13] J. C. Slonczewski, Phys. Rev. B **39**, 6995 (1989).
[14] W. E. Pickett and D. J. Singh, Phys. Rev. B **53**, 1146 (1996).
[15] A. J. Millis, P. B. Littlewood, and B. I. Shraiman, Phys. Rev. Lett. **74**, 5144 (1995).
[16] Gang Xiao, C. L. Chien, and M. Natan, J. Appl. Phys. **61**, 3246 (1987).
[17] R. Wiesendanger, H.-J. Guntherodt, G. Guntherodt, R. J. Gambino, and R. Ruf, Phys. Rev. Lett. **65**, 247 (1990).